Supplementary information

Aqueous synthesis of $Na_{3-2x}Sb_{1-x}W_xS_{4-x}I_x$ solid-state electrolytes with ultrahigh ionic conductivity

Yuxin Shao[1,2,3,#], Chengwei Gao[1,2,3,#,], Chengmiao He[1,2,3], Zipeng Liu[1,2,3], Lanlan Xing[1,2,3], Zhenyu Zhang[1,2,3], Shiliang Kang[1,2,3], Linling Tan[1,2,3], Qing Jiao[1,2,3], Ying Xie[1,2,3], Yanfei Zhang[4], Baoan Song[1,2,3], Shixun Dai[1,2,3], Yuanzheng Yue[5,*], Changgui Lin[1,2,3,*]*

[1]*Laboratory of Infrared Materials and Devices, The Research Institute of Advanced Technologies, Ningbo University, Ningbo, 315211, China*

[2]*Key Laboratory of Photoelectric Detection Materials and Devices of Zhejiang Province, Ningbo University, Ningbo, 315211, China*

[3]*Engineering Research Center for Advanced Infrared Photoelectric Materials and Devices of Zhejiang Province, Ningbo University, Ningbo, 315211, China*

[4] *School of Materials Science and Engineering, Qilu University of Technology (Shandong Academy of Sciences), Jinan 250353, China*

[5] *Department of Chemistry and Bioscience, Aalborg University, DK-9220 Aalborg, Denmark*

E-mails: C. W. Gao (gaochengwei@nbu.edu.cn), Y. Z. Yue (yy@bio.aau.dk); C. G. Lin (linchanggui@nbu.edu.cn)

Supplementary Figure 1-3 are synthesis and structure of the Na_3SbS_4, $Na_3SbS_{4-x}I_x$ and $Na_{3-2x}Sb_{1-x}W_xS_{4-x}I_x$ (x=0.05, 0.1 ,0.15) SSEs.

Supplementary Table 1 is the crystallographic data for the prepared $Na_{2.8}Sb_{0.9}W_{0.1}S_{3.9}I_{0.1}$.

Supplementary Table 2-3 are the EDS and ICP-MS data for the prepared $Na_{2.8}Sb_{0.9}W_{0.1}S_{3.9}I_{0.1}$.

Supplementary Figure 4 is the apparent density of $Na_{2.8}Sb_{0.9}W_{0.1}S_{3.9}I_{0.1}$ SSEs.

Supplementary Figure 5-6 are conduction characteristics of the Na_3SbS_4, $Na_3SbS_{4-x}I_x$ and $Na_{3-2x}Sb_{1-x}W_xS_{4-x}I_x$ (x=0.05, 0.1 ,0.15) SSEs.

Supplementary Figure 7-8 are chemical stability characteristic of the $Na_{3-2x}Sb_{1-x}W_xS_{4-x}I_x$ (x=0.05, 0.1 ,0.15), Na_3SbS_4, Na_3PS_4 and Li_6PS_5Cl.

Supplementary Table 4 is the summary of chemical stability characteristic for the $Na_{2.8}Sb_{0.9}W_{0.1}S_{3.9}I_{0.1}$, Na_3SbS_4, Na_3PS_4 and Li_6PS_5Cl.

Supplementary Figure 9-11 are solid-state battery performance of $Na_{3-2x}Sb_{1-x}W_xS_{4-x}I_x$ (x=0.05, 0.1 ,0.15) SSEs.

Supplementary Figure 12 is the element mapping of Na, Sb, S, W, I, Ti of the aqueous synthesis anode.

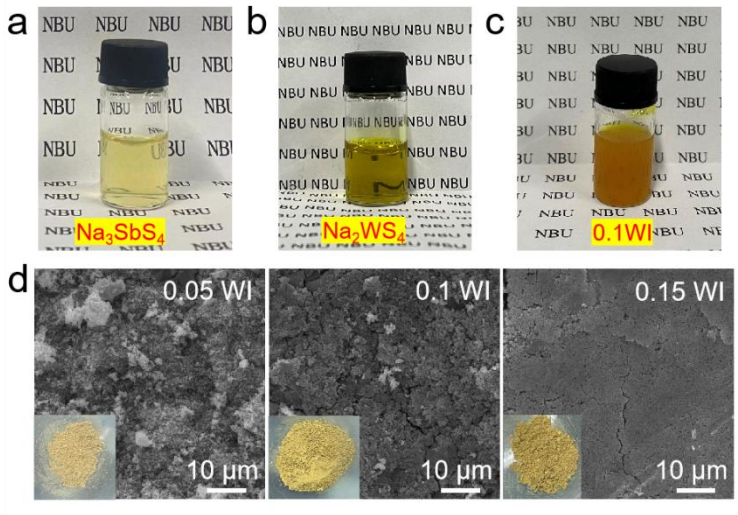

Supplementary Figure 1. Optical images of the precursor aqueous solutions of **a** Na_3SbS_4, **b** Na_2WS_4 and **c** 0.1WI. **d** Backscattered electron (BSE) images of $Na_{3-2x}Sb_{1-x}W_xS_{4-x}I_x$ SSEs (x=0.05, 0.1 ,0.15) with a scale bar of 10 μm. The insert shows the heat-treated powders optical images.

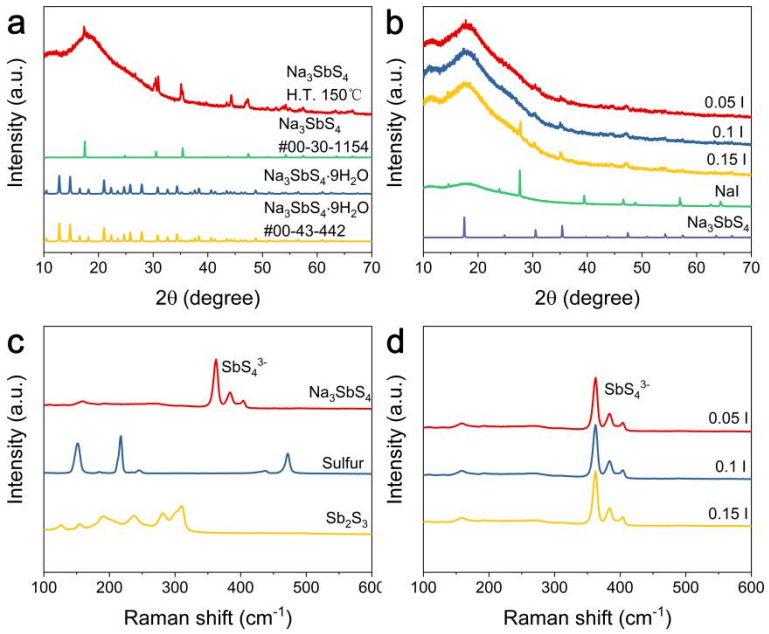

Supplementary Figure 2. a-b XRD patterns of $Na_3SbS_4·9H_2O$, Na_3SbS_4 and $Na_3SbS_{4-x}I_x$ (x=0.05, 0.1, 0.15) prepared by the aqueous phase method. **c-d** Raman spectra of Na_3SbS_4, sulfur, Sb_2S_3 and $Na_{3-2x}SbS_{4-x}I_x$ (x=0.05, 0.1, 0.15).

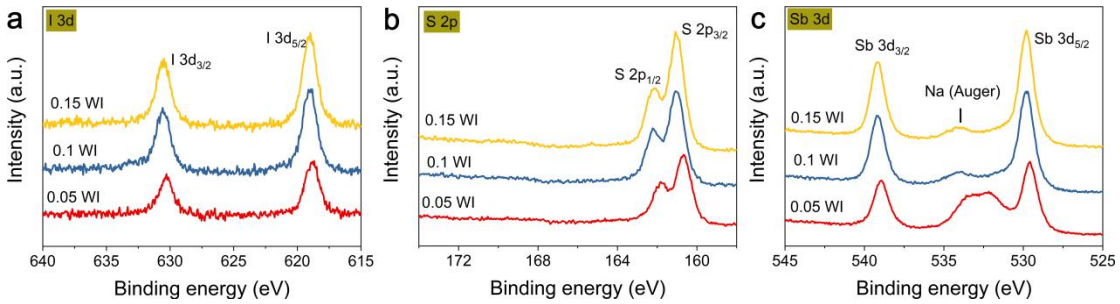

Supplementary Figure 3. XPS core levels of **a** I 3d, **b** S 2p and **c** Sb 3d of $Na_{3-2x}Sb_{1-x}W_xS_{4-x}I_x$ SSEs (x=0.05, 0.1 ,0.15).

Table S1. Crystallographic data for the prepared $Na_{2.8}Sb_{0.9}W_{0.1}S_{3.9}I_{0.1}$.

Crystal System	Cubic		Lattice Parameter		a = 7.199198 Å	
Space Group	*I*-43m (No. 217)		Volume, Z		V = 373.123 Å^3, Z = 2	
Atoms						
x y z B / Å2	Wyckoff	Occupancy	x	y	z	B/Å^2
Na	6*b*	0.933	0	0	1/2	
Sb	2*a*	0.9	0	0	0	
W	2*a*	0.1	0	0	0	
S	8*c*	0.975	0.191947(1)	0.191947(1)	0.191947(1)	
I	8*c*	0.025	0.191947(1)	0.191947(1)	0.191947(1)	

*R_{wp} = 0.0238, R_p = 0.0353

Table S2. EDS (Energy Dispersive Spectrometer) data for the $Na_{2.8}Sb_{0.9}W_{0.1}S_{3.9}I_{0.1}$ SSE.

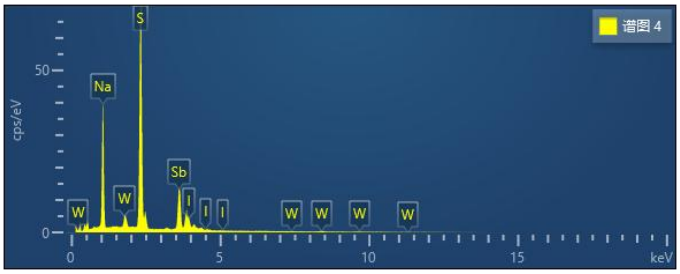

Element	Series	Weight wt. %	Atomic at. %	Error
Na	K-series	19.96	37.20	0.18
Sb	L-series	35.79	12.59	0.30
W	L-series	5.13	1.20	0.22
S	L-series	35.85	47.90	0.24

I	K-series	3.27	1.10	0.0.3

Table S3. ICP-MS (Inductively Coupled Plasma Mass Spectrometry) data for $Na_{2.8}Sb_{0.9}W_{0.1}S_{3.9}I_{0.1}$ SSE.

Weight m_0 (g)	Constant volume V_0 (ml)	Element	Test solution element concentration C_0 (ug/L)	Dilution factor f	Element concentration C_1 in the original digestion solution (ug/L)	Element content C_x (ug/kg)	Element content W (%)
0.0559	25	I	184.7691	500	92384.5250	41316871.6458	4.1317%
0.0559	25	I	187.3601	500	93680.0400	41896261.1807	4.1896%
0.0559	25	I	185.8926	500	92946.2950	41568110.4651	4.1568%
0.0457	25	Na	35.4451	10	354.4505	193900.7265	19.3901%
0.0457	25	Na	35.4212	10	354.2124	193770.4590	19.3770%
0.0457	25	Na	35.5059	10	355.0586	194233.3549	19.4233%
0.0457	25	S	5.9626	100	596.2628	326183.1260	32.6183%
0.0457	25	S	6.0781	100	607.8101	332500.0728	33.2500%
0.0457	25	S	6.0054	100	600.5418	328523.9422	32.8524%
0.0457	25	Sb	6.0316	100	603.1640	329958.4333	32.9958%
0.0457	25	Sb	6.0747	100	607.4650	332311.2888	33.2311%

0.0457	25	Sb	6.0782	100	607.8247	332508.0246	33.2508%
0.0457	25	W	1.2379	100	123.7877	67717.5870	6.7718%
0.0457	25	W	1.2560	100	125.6025	68710.3364	6.8710%
0.0457	25	W	1.2531	100	125.3067	68548.5498	6.8549%

$$C_x = C_0 * f * 10^{-3} / m_0 * 10^{-3} = C_1 * V_0 \quad (1)$$

$$w = C_x / 10^9 * 100\% \quad (2)$$

The corresponding standard series curves of I, Na, S, Sb and W, respectively are shown below.

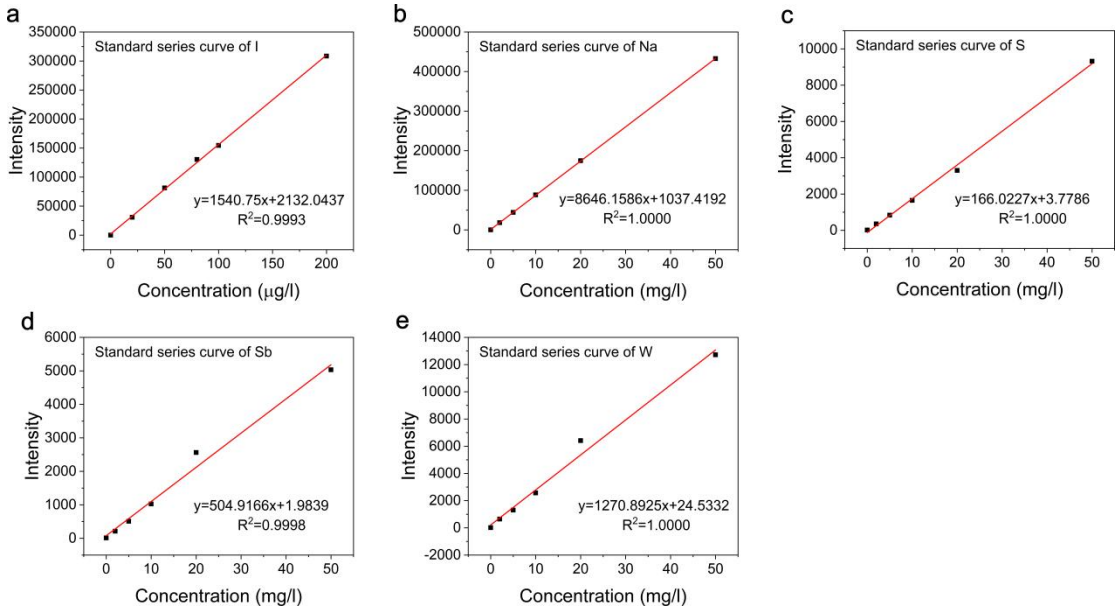

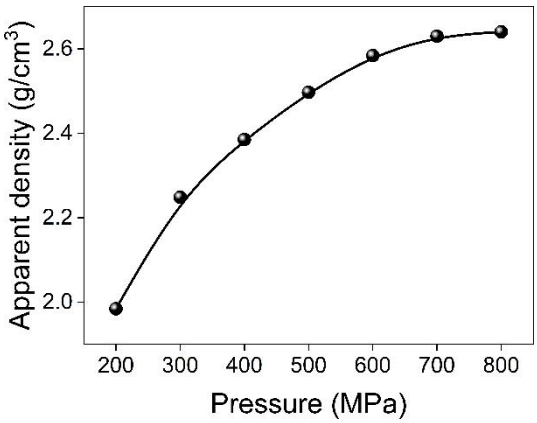

Supplementary Figure 4. Apparent density of $Na_{2.8}Sb_{0.9}W_{0.1}S_{3.9}I_{0.1}$ SSEs. The apparent density area at ~2.6 g cm-3 when the pressure ≥ 700 MPa.

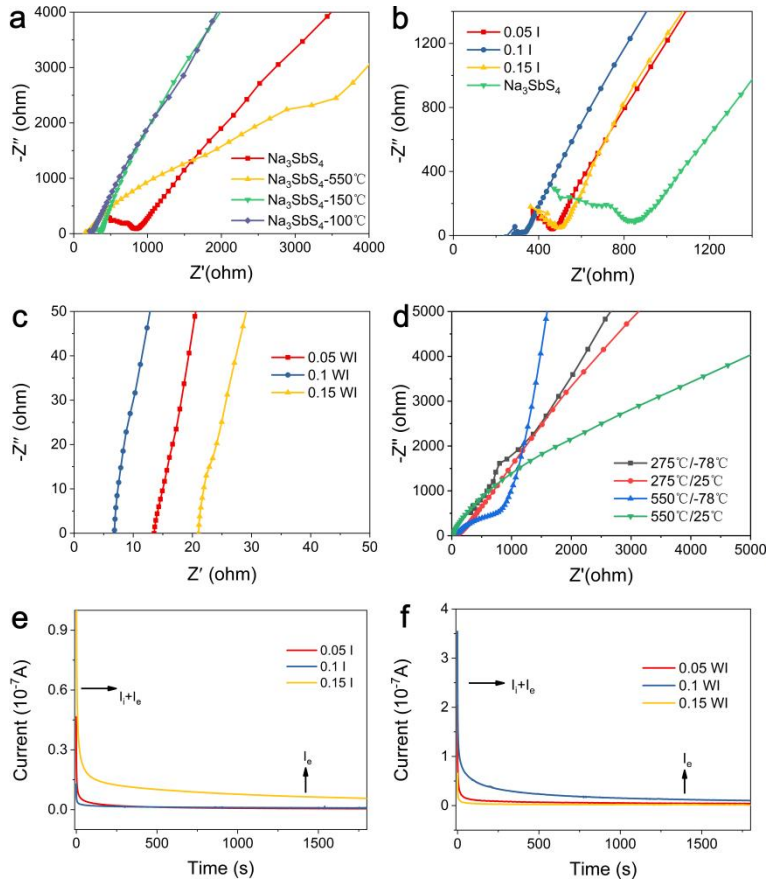

Supplementary Figure 5. a Nyquist plots of Na_3SbS_4 were cold pressed at 720 MPa, annealed at 550 ℃, 150℃ and 100 ℃, respectively. The yellow curve of Na_3SbS_4 was prepared by solid phase method. **b-c** Nyquist plots of $Na_3SbS_{4-x}I_x$ and $Na_{3-2x}Sb_{1-x}W_xS_{4-x}I_x$ SSEs (x=0.05, 0.1 ,0.15), respectively. **d** Nyquist plots of $Na_{2.8}Sb_{0.9}W_{0.1}S_{3.9}I_{0.1}$ at -78 °C and room temperature (25 °C) after heat treatment at 275 °C and 550 °C, respectively. **e-f** Direct current polarization curves of $Na_{3-2x}SbS_{4-x}I_x$ and $Na_{3-2x}Sb_{1-x}W_xS_{4-x}I_x$ SSEs (x=0.05, 0.1 ,0.15), respectively.

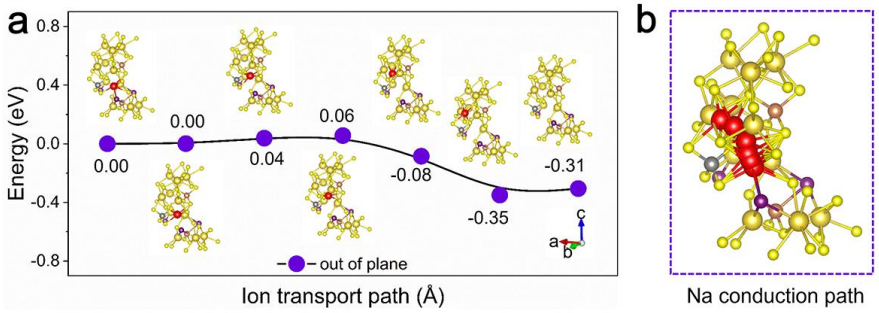

Supplementary Figure 6. a Activation energy barriers for sodium ion migration and **b** the theoretically obtained structure model for the ground state of the $Na_{2.8}Sb_{0.9}W_{0.1}S_{3.9}I_{0.1}$ and with the marked sodium ion migration path corresponding.

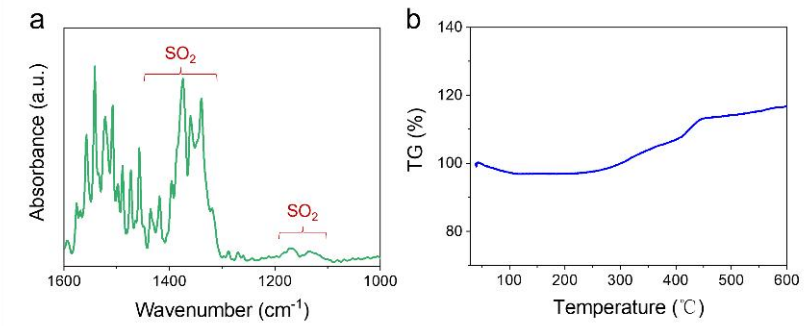

Supplementary Figure 7. a FTIR spectra of $Na_{2.8}Sb_{0.9}W_{0.1}S_{3.9}I_{0.1}$ in the pure oxygen atmosphere, the formation of SO_2 is evidenced by the bands at 1450-1300 and 1150 cm^{-1}. **b** The corresponding TG of TG-IR at a heating rate of 10 ℃/min.

Table S4. Summary of the enthalpies, Gibbs Energies and bond energy of Formation for Sb-O, Sb-S, W-O, W-S, P-O and P-S at 298.15 K, respectively.

Bond	Δ_fH° (kJ/mol)	Δ_fG° (kJ/mol)	Bond Energy(kJ/mol)
Sb-O (Sb_2O_3)	-708.8	-831.0	372.0 (84)
Sb-S (Sb_2S_3)	-174.9	-174.9	379.0
W-O (WO_3)	-842.9	-764.1	635.0 (25)
W-S (WS_2)	-243.1	-23.0	440.0
P-O (P_2O_5)	-2984.0	-2697.7	596.0
P-O (P_2S_5)	-1770.0	-1506	346.0 (17)

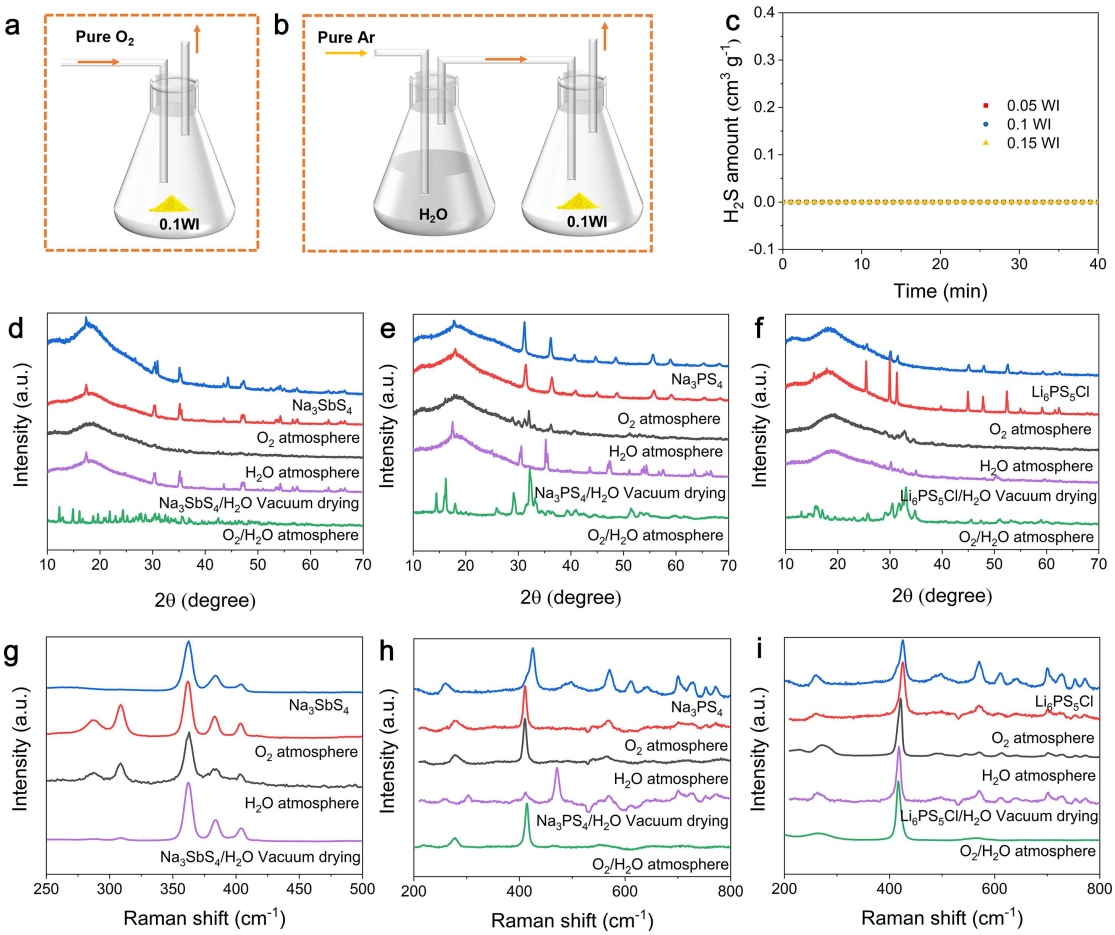

Supplementary Figure 8. a-b Schematic diagram of controlled humidity exposure experiments with continuous O_2 and H_2O purging for 12 h. **c** The amount of H_2S released by $Na_{3-2x}Sb_{1-x}W_xS_{4-x}I_x$ SSEs (x=0.05, 0.1 ,0.15) exposed to moist air for 40 min. **d-f** XRD and **g-i** Raman spectroscopy before and after exposure experiments in specific atmosphere of Na_3SbS_4, Na_3PS_4 and Li_6PS_5Cl, respectively.

Table S5. Summary of O_2, H_2O and the mixture of O_2/H_2O stability of several typical chalcogenide electrolytes.

Atmosphere	0.1WI	Na_3SbS_4	Na_3PS_4	Li_6PS_5Cl
O_2	X	X	√	√
H_2O	√	√	X	√
O_2/H_2O	X	X	X	X

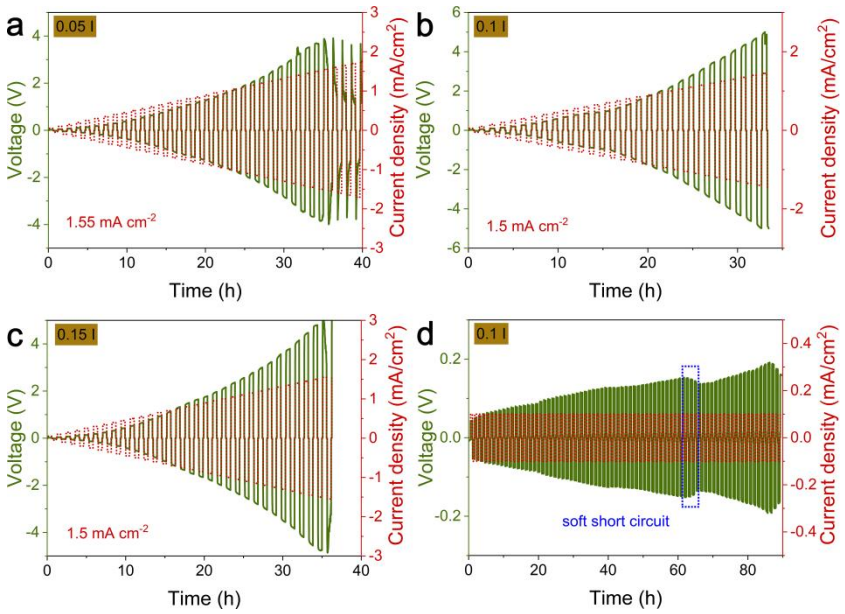

Supplementary Figure 9. a-c Critical current density tests of the Na|SSEs|Na symmetric cells at step-increased current densities at room temperature where SSEs are $Na_3SbS_{4-x}I_x$ (x=0.05, 0.1, 0.15), respectively. The time for each charge and discharge step is 0.5 h. The step size for the current increase is 0.05 mA cm^{-2}. **d** Galvanostatic sodium striping/plating cycling of the Na|$Na_{2.8}SbS_{3.9}I_{0.1}$|Na symmetric cells at 0.1 mA cm^{-2} at room temperature. The time for each striping and plating segment is 0.5 h.

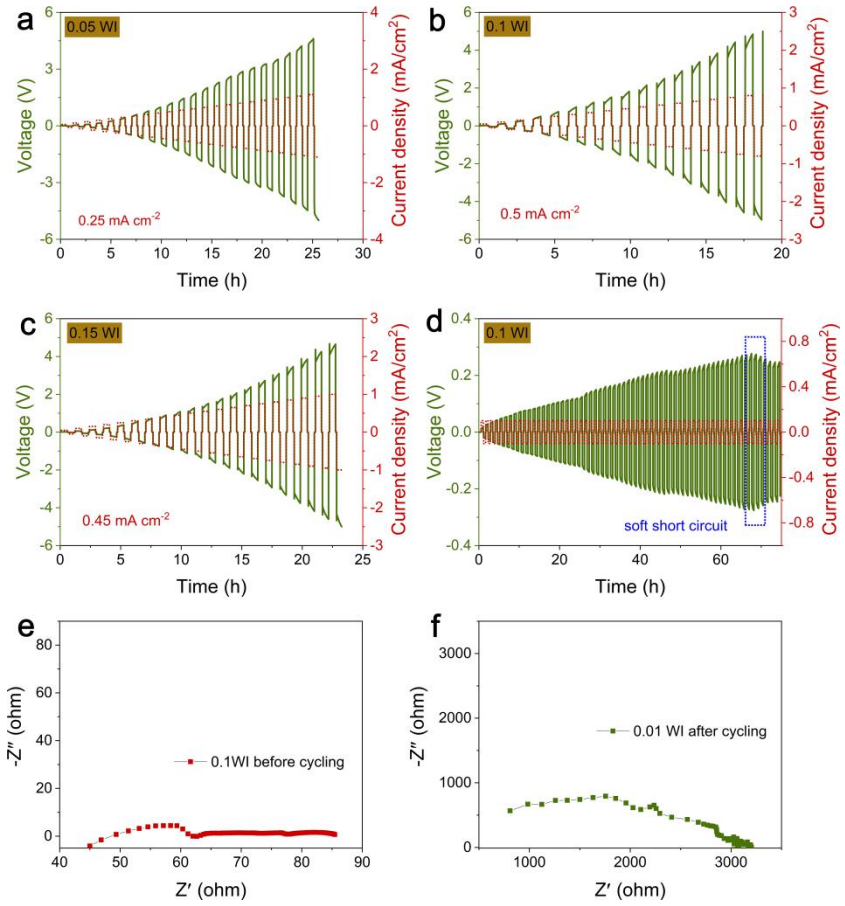

Supplementary Figure 10. a-c Critical current density tests of the Na|SSEs|Na symmetric cells at step-increased current densities at room temperature where SSEs are $Na_{3-2x}Sb_{1-x}W_xS_{4-x}I_x$ (x=0.05, 0.1, 0.15), respectively. **d** Galvanostatic sodium striping/plating cycling of the Na|$Na_{2.8}Sb_{0.9}W_{0.1}S_{3.9}I_{0.1}$|Na symmetric cells at 0.1 mA cm^{-2}. **e-f** Nyquist plots of Na|$Na_{2.8}Sb_{0.9}W_{0.1}S_{3.9}I_{0.1}$|Na before and after cycling.

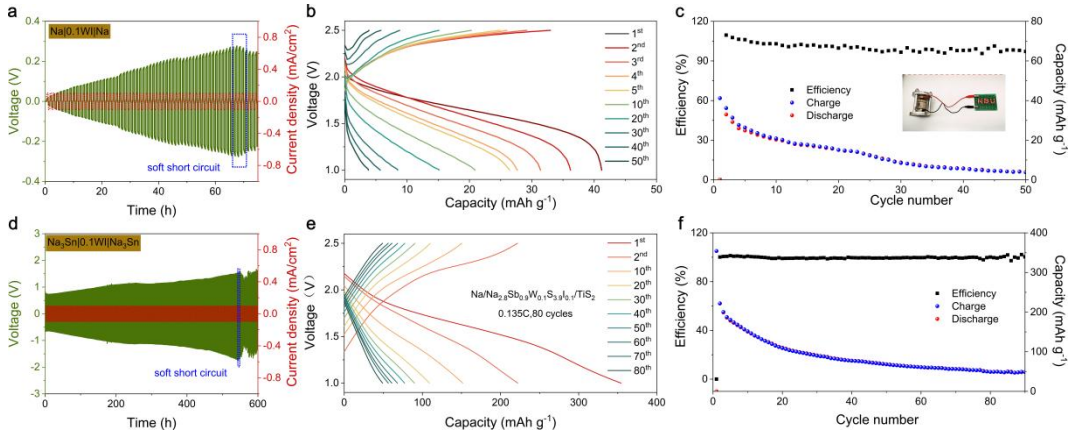

Supplementary Figure 11. a and **d** Galvanostatic sodium striping/plating cycling of the Na|$Na_{2.8}Sb_{0.9}W_{0.1}S_{3.9}I_{0.1}$|Na and Na_3Sn|$Na_{2.8}Sb_{0.9}W_{0.1}S_{3.9}I_{0.1}$|$Na_3Sn$ symmetric cells at 0.1 mA cm^{-2}. **b** Galvanostatic voltage profile and **c** galvanostatic cycling

performance of the Na|$Na_{2.8}Sb_{0.9}W_{0.1}S_{3.9}I_{0.1}$|$TiS_2$ full cell. The insert is a light bulb demonstration after the battery is assembled. **e** Galvanostatic voltage profile and **f** galvanostatic cycling performance of the Na_3Sn|$Na_{2.8}Sb_{0.9}W_{0.1}S_{3.9}I_{0.1}$|$TiS_2$ full cell.

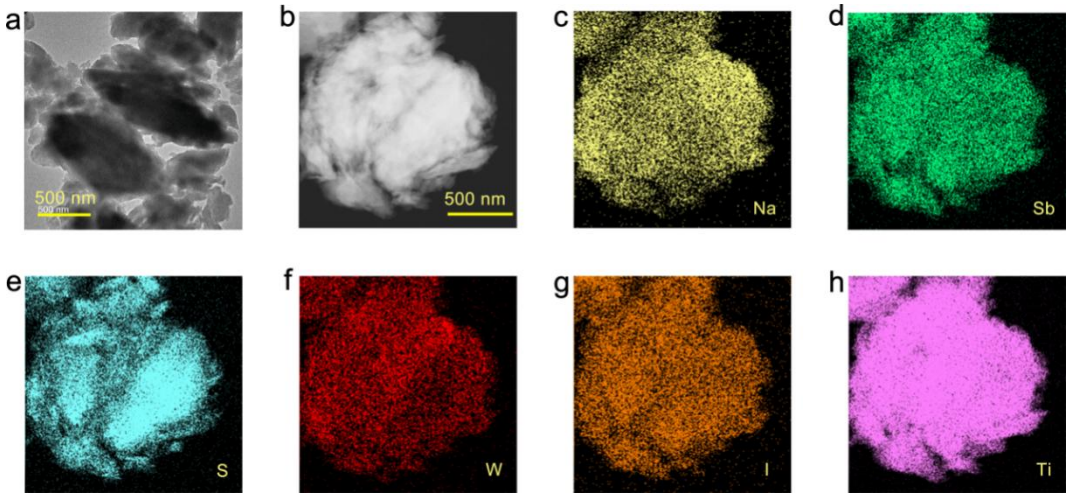

Supplementary Figure 12. Element mapping of Na, Sb, S, W, I, Ti of the aqueous synthesis anode.